



Carbon export from leaves is controlled via ubiquitination and phosphorylation of sucrose transporter SUC2

Qiyu Xu^{a,b}, Shijiao Yin^{a,b}, Yue Ma^{a,b}, Min Song^{a,b}, Yingjie Song^a, Shuaicheng Mu^a, Yunsong Li^a, Xiaohui Liu^{a,b}, Yunjuan Ren^{a,b}, Chen Gao^{a,b}, Shaolin Chen^{a,b}, and Johannes Liesche^{a,b,1} 

^aCollege of Life Sciences, Northwest A&F University, 712100 Yangling, China; and ^bBiomass Energy Center for Arid and Semi-Arid Lands, Northwest A&F University, 712100 Yangling, China

Edited by Mark Stitt, Max-Planck-Institut für Molekulare Pflanzenphysiologie, Golm, Germany, and accepted by Editorial Board Member Joseph R. Ecker February 3, 2020 (received for review July 24, 2019)

All multicellular organisms keep a balance between sink and source activities by controlling nutrient transport at strategic positions. In most plants, photosynthetically produced sucrose is the predominant carbon and energy source, whose transport from leaves to carbon sink organs depends on sucrose transporters. In the model plant *Arabidopsis thaliana*, transport of sucrose into the phloem vascular tissue by SUCROSE TRANSPORTER 2 (SUC2) sets the rate of carbon export from source leaves, just like the SUC2 homologs of most crop plants. Despite their importance, little is known about the proteins that regulate these sucrose transporters. Here, identification and characterization of SUC2-interaction partners revealed that SUC2 activity is regulated via its protein turnover rate and phosphorylation state. UBIQUITIN-CONJUGATING ENZYME 34 (UBC34) was found to trigger turnover of SUC2 in a light-dependent manner. The E2 enzyme UBC34 could ubiquitinate SUC2 *in vitro*, a function generally associated with E3 ubiquitin ligases. *ubc34* mutants showed increased phloem loading, as well as increased biomass and yield. In contrast, mutants of another SUC2-interaction partner, WALL-ASSOCIATED KINASE LIKE 8 (WAKL8), showed decreased phloem loading and growth. An *in vivo* assay based on a fluorescent sucrose analog confirmed that SUC2 phosphorylation by WAKL8 can increase transport activity. Both proteins are required for the up-regulation of phloem loading in response to increased light intensity. The molecular mechanism of SUC2 regulation elucidated here provides promising targets for the biotechnological enhancement of source strength.

carbon allocation | phloem loading | sucrose transporter | posttranslational regulation | *Arabidopsis*

In a multicellular organism, growth, development, acclimation, and homeostasis require mechanisms that monitor changes in the environment, coordinate reactions in cells and compartments, and adjust transport of ions and metabolites across cellular membranes. In plants, this entails control of the flux of sucrose, the predominant unit of carbon and energy (1). Sucrose is produced in photosynthetically active tissues of the leaf and stem and transported to carbon sink organs in the highly specialized cells of the phloem vascular system. Since transport inside the phloem happens by osmotically driven mass flow, it is the loading and unloading reactions that determine the transport rate (2). In most crops and the model plant *Arabidopsis thaliana*, phloem loading is mediated by secondary active SUCROSE TRANSPORTERS (SUCs or SUTs) after sucrose secretion into the cell-wall space by passive SUGARS WILL EVENTUALLY BE EXPORTED TRANSPORTERS (SWEETs) from cells surrounding the phloem (3). Unloading happens mostly by diffusion through plasmodesmata (4). This arrangement makes SUCs the most likely target of regulation. Indeed, recent analysis of phloem transport in response to environmental cues suggested that carbon export from leaves is directly linked to SUC activity (5–7).

Despite their strategic role in whole-plant carbon partitioning, relatively little is known about the mechanism of regulation of

SUCs responsible for phloem loading. Gene expression was found to scale with phloem loading in response to certain abiotic stresses (5–7), but did not scale with phloem loading in response to increased light levels (7). In tomato, increased phloem loading under high-light conditions coincided with increased protein abundance of the phloem-loading SUC instead, indicating posttranscriptional regulation (7). Transcriptional and posttranscriptional regulation of the phloem-loading SUC was also observed in sugar beet in response to exogenously fed sucrose (8, 9).

Different mechanisms of posttranscriptional regulation of SUCs have been suggested previously. The redox state of potato StSUT1 was shown to influence homodimerization and protein localization when expressed in yeast, although seemingly without affecting transport activity (10). StSUT1-GFP expressed in tobacco epidermal cells showed constant endocytosis and recycling, which could potentially serve the regulation of the number of transporters at the plasma membrane (11). A correlation of protein abundance with measured transport activity and a fast turnover rate was found for the phloem-loading SUC of sugar beet, BvSUT1 (9). The interaction of the SUC and other proteins has been described, but without demonstrating any direct effects on

Significance

Plants depend on strict regulation of carbon transport to keep the activities of different parts in balance under various environmental conditions. In most crops and the model plant *Arabidopsis thaliana*, sucrose transporters (SUCs) that are strategically positioned in the leaf veins are responsible for carbon export from photosynthetically active leaves. Despite their central role, relatively little is known about the regulation of SUCs. This study identified two regulatory proteins of *Arabidopsis* SUC2 and investigated how they modulate sucrose transport activity. Both proteins proved important for the environmental acclimation of leaf carbon export. Furthermore, the increased biomass and yield of plants lacking a regulator observed here demonstrate that manipulation of SUC regulation can be a viable path to enhance plant productivity.

Author contributions: Q.X. and J.L. designed research; Q.X., S.Y., Y.M., M.S., Y.S., S.M., Y.L., X.L., Y.R., and C.G. performed research; S.C. and J.L. contributed new reagents/analytic tools; Q.X., S.Y., and J.L. analyzed data; and Q.X. and J.L. wrote the paper.

The authors declare no competing interest.

This article is a PNAS Direct Submission. M.S. is a guest editor invited by the Editorial Board.

This open access article is distributed under [Creative Commons Attribution-NonCommercial-NoDerivatives License 4.0 \(CC BY-NC-ND\)](https://creativecommons.org/licenses/by-nc-nd/4.0/).

See [online](#) for related content such as Commentaries.

¹To whom correspondence may be addressed. Email: liesche@nwafu.edu.cn.

This article contains supporting information online at <https://www.pnas.org/lookup/suppl/doi:10.1073/pnas.1912754117/-DCSupplemental>.

First published March 2, 2020.

sucrose transport activity (12–15). Kinase activity influences the abundance of BvSUT1, either through phosphorylation of the transporter itself or of regulatory proteins (16). For SUCs that are not involved in phloem loading, such as apple MdSUT2.2, regulation via phosphorylation has been shown (15, 17–21).

The aim of this study was to elucidate the molecular mechanism of posttranscriptional regulation of SUC2, the phloem-loading SUC of *Arabidopsis* (22–24). It was tested if SUC2 is regulated by phosphorylation or by processes that affect protein abundance, namely messenger RNA (mRNA) translation efficiency and protein turnover. Candidates for SUC2-regulating proteins were obtained from a recent membrane protein interactomics screen that used the mating-based yeast two-hybrid system (25). The investigation was facilitated by employment of a recently developed SUC2-transport assay based on the fluorescent sucrose-analog esculin, which allows probing the influence of protein modifications on transport activity in vivo, in plant cells (26).

Results

Increased Phloem Loading Coincides with Decreased SUC2 Protein Turnover Rate and Increased Phosphorylation. Comparison of *Arabidopsis* plants grown under normal light ($90 \mu\text{mol photon}\cdot\text{m}^{-2}\cdot\text{s}^{-1}$) with those exposed to high-light conditions ($400 \mu\text{mol photon}\cdot\text{m}^{-2}\cdot\text{s}^{-1}$) for 4 h was used as the main experimental paradigm to investigate SUC2 regulation. Transfer to high light increased photosynthesis, soluble leaf sugar levels, and sucrose content of the phloem, while *SUC2* gene expression remained unchanged (Fig. 1A). Anti-SUC2 antibodies were used for Western blots, which showed that SUC2 protein abundance increased in line with the increased phloem sucrose content (Fig. 1A and *SI Appendix*, Fig. S1).

The increase in the protein-to-mRNA ratio could be due to increased SUC2 translation or to reduced protein turnover. Translation efficiency was assessed here by polysome profiling. Quantification of total mRNAs showed no significant difference in the number of mRNAs bound to monosomes and polysomes of plants exposed to normal- or high-light conditions (Fig. 1B). Similarly, no significant difference was found for SUC2 mRNA

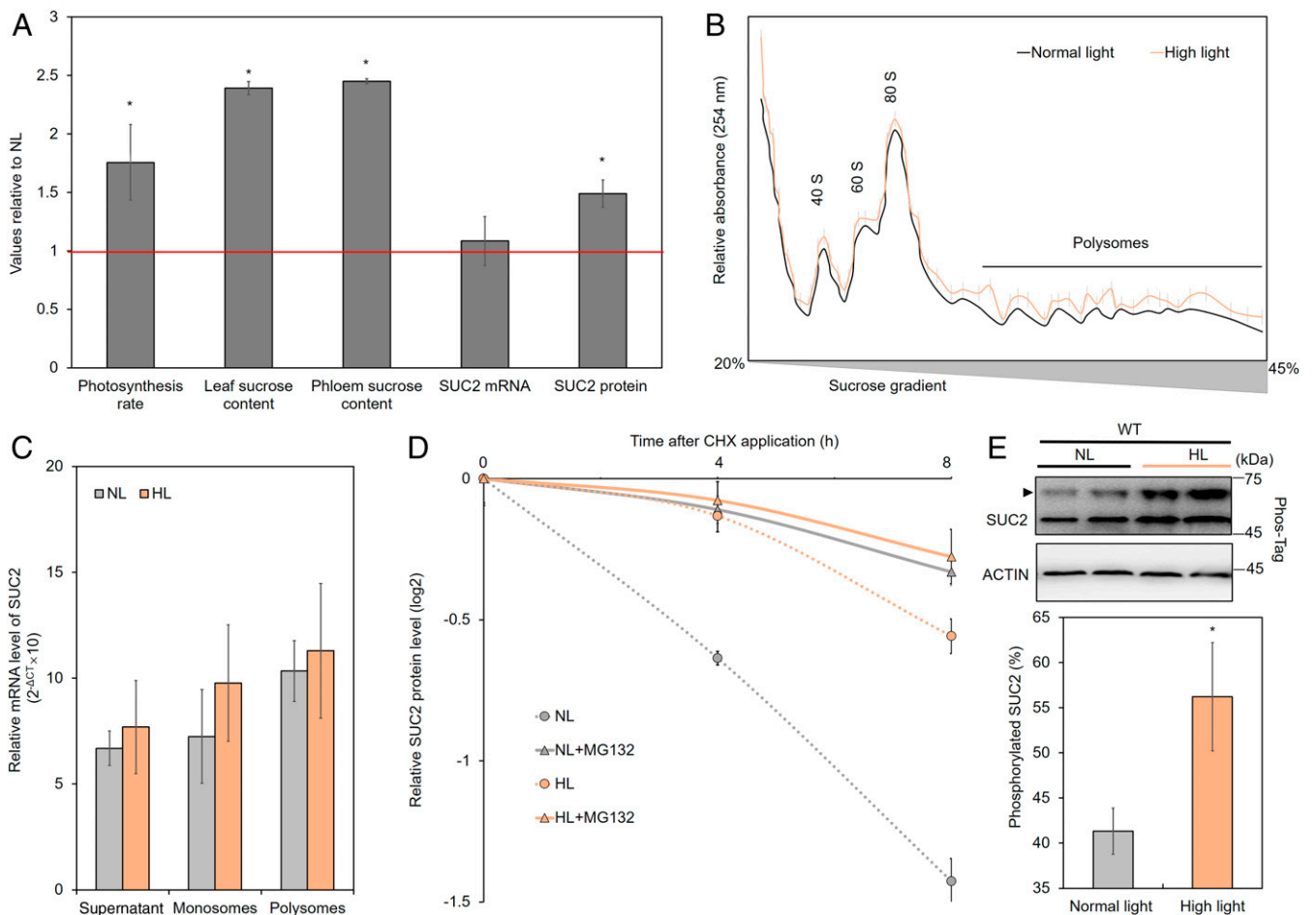


Fig. 1. Posttranscriptional regulation of SUC2. (A) Photosynthesis rate, leaf and phloem sucrose content, *SUC2* expression, and SUC2 protein abundance in rosette leaves of 3-wk-old *Arabidopsis* seedlings exposed to high-light (HL) conditions for 4 h relative to values obtained from seedlings grown under normal light (NL). The same sample type and treatment were used to generate all data shown in this figure. (B) Optical density profiles of polysome gradient fractions from plants exposed to NL or HL conditions indicating the number of mRNAs associated with monosomes (40S, 60S, and 80S) and polysomes. (C) Number of *SUC2* mRNAs associated with monosomes or polysomes or in solution (supernatant) measured by qPCR. UBQ10 and ACTIN12 were used as internal controls. (D) Relative *SUC2* protein levels after application of the protein synthesis inhibitor CHX alone or CHX and the inhibitor of membrane protein turnover MG132 for 4 and 8 h. (E, Upper) Immunoblot analysis with a *SUC2* antibody using Phos-Tag SDS/PAGE. Phos-Tag selectively hinders the movement of phosphorylated protein in the gel, leading to separate bands for phosphorylated and unphosphorylated proteins. The arrowhead indicates the band of phosphorylated *SUC2* protein. Molecular mass is indicated (Right) in kilodaltons (kDa). (E, Lower) The amount of phosphorylated *SUC2* relative to the total amount of *SUC2*. Concentrations of all major leaf and phloem sugars, as well as representative Western blot images, are displayed in *SI Appendix*, Fig. S1. Significant differences ($P < 0.05$) are indicated by an asterisk. All error bars represent SD from the mean ($n = 3$ [A–C and E], 4 [D], and 5 [*SUC2* protein in A]). WT, wild type.

(Fig. 1C), indicating a similar translation efficiency under high-light and normal-light conditions. In contrast, SUC2 turnover rate was found to change with light level. After inhibition of protein synthesis through application of cycloheximide (CHX), SUC2 abundance decreased at a lower rate under high-light conditions than under control conditions (Fig. 1D and *SI Appendix, Fig. S1*).

Turnover of SUC2, as a membrane-integral protein, can be assumed to happen via ubiquitin-dependent sorting to the vacuole (27). This was tested by application of CHX in conjunction with MG132, which interferes with targeting of membrane proteins to the vacuole (28). Coapplication of CHX and MG132 reduced SUC2 turnover rate to less than 5% per hour and no significant difference was observed between normal- and high-light conditions (Fig. 1D and *SI Appendix, Fig. S1*), indicating that modulation of the rate of SUC2 turnover is part of the plant's high-light acclimation response.

In addition, it was tested if SUC2 can be phosphorylated and if the phosphorylation level is influenced by light intensity using the Phos-Tag assay. The Phos-Tag reagent binds to phosphorylated ions, thereby delaying the migration of phosphorylated proteins on a sodium dodecyl sulfate (SDS) polyacrylamide gel. Using the anti-SUC2 antibody, an additional band corresponding to a higher molecular mass was observed on a Phos-Tag SDS polyacrylamide gel, which significantly increased in strength in samples from high light-treated plants (Fig. 1E and *SI Appendix, Fig. S1*). The additional band disappeared after treatment with alkaline phosphatase for 1 h (*SI Appendix, Fig. S1H*), confirming that it corresponds to phosphorylated SUC2 protein.

Ubiquitin-Conjugating Enzyme UBC34 Interacts with SUC2. The yeast two-hybrid assay of *Arabidopsis* membrane proteins performed by Jones et al. (25) provided a number of potential interaction partners of SUC2. One of these showed a clear association with the protein-turnover pathway, UBIQUITIN-CONJUGATING ENZYME 34 (UBC34). In order to verify the interaction of SUC2 and UBC34, we performed Förster resonance energy transfer (FRET) and glutathione S-transferase (GST) pull-down experiments. FRET acceptor bleaching was conducted with SUC2 coupled to monomeric Turquoise 2 (mT2) as donor and UBC34 coupled to yellow fluorescent protein (YFP) as acceptor, coexpressed in *Nicotiana benthamiana* leaf epidermal cells. SUC2-mT2 coexpressed with SUC3-YFP was used as positive control and SUC2-mT2 coexpressed with STP1-YFP as negative control. Photobleaching of the acceptor (YFP) yielded a significant increase in fluorescence of the donor (mT2) for SUC2-SUC3 but not for SUC2-STP1 (*SI Appendix, Fig. S2*). Photobleaching of UBC34-YFP led to an increase in fluorescence signal of SUC2-mT2 (*SI Appendix, Fig. S2*), resulting in FRET efficiencies similar to the positive control and significantly higher than the negative control (Fig. 2A).

To test if SUC2 and UBC34 can directly bind to each other, we also performed GST pull-down assays, for which truncations of UBC34 lacking the C-terminal transmembrane domain were made to enhance solubility. This GST-UBC34 Δ tmd was expressed in *Escherichia coli*, extracted, and purified (Fig. 2B and *SI Appendix, Fig. S3*). GST-UBC34 Δ tmd immobilized on glutathione-Sepharose beads was incubated with leaf membrane proteins. As a negative control, GST alone immobilized on beads was incubated with the same leaf proteins. Compared with the control group, the GST-UBC34 Δ tmd fusion protein readily pulled down SUC2 from the leaf membrane proteins (Fig. 2C), demonstrating the potential for direct interaction.

Since SUC2 is expressed exclusively in the phloem, the tissue specificity of UBC34 expression was explored. Transcriptomics data from *Arabidopsis* rosette leaves showed that UBC34 is expressed in a diverse set of leaf tissues, including the phloem (Fig. 2D).

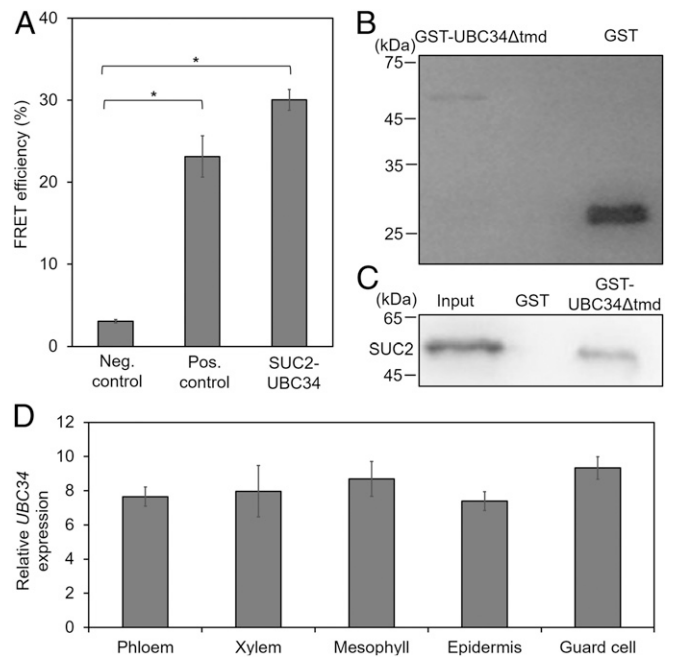


Fig. 2. Protein-protein interaction of UBC34 and SUC2. (A) FRET efficiency of SUC2-mT2 and UBC34-YFP compared with the efficiency of the negative control SUC2-mT2 and STP1-YFP and the positive control SUC2-mT2 and SUC3-YFP. (B) Purified recombinant GST and GST-UBC34 Δ tmd proteins used in the GST pull-down assay visualized using an anti-GST antibody. Numbers (Left) indicate molecular mass (kDa). (C) Immunoblot using an anti-SUC2 antibody showing bands for SUC2 in the total protein extract that was used as input for the pull-down assay, as well as in the proteins after pull down with GST-UBC34 Δ tmd-bound beads. GST alone was used as the negative control. (D) Relative gene expression of UBC34 in different tissues of rosette leaves. FRET images are displayed in *SI Appendix, Fig. S2* and blots related to protein purification are in *SI Appendix, Fig. S3*. Asterisks indicate significant differences ($P < 0.05$). All error bars depict SD of the mean ($n = 6$ [D] and 7 [A]).

UBC34 Controls Light-Dependent Turnover Rate of SUC2. Homozygous mutants with a T-DNA insertion mutation in the exon of UBC34 were selected using PCR-based genotyping and verified by qRT-PCR analysis (*SI Appendix, Fig. S4*). *ubc34* mutant plants showed higher SUC2 protein levels while SUC2 expression did not significantly differ from wild-type levels (Fig. 3A). Sucrose levels in the soluble leaf sugar fraction and in the phloem exudate were significantly increased compared with wild-type levels (Fig. 3A). Of the other soluble sugars common in leaves, glucose also showed a significant increase, while fructose and maltose levels were similar between wild type and *ubc34* mutant (*SI Appendix, Fig. S5*). Furthermore, photosynthesis rate, rosette diameter, fresh and dry weight, seed weight, and starch content of *ubc34* plants were all increased, while no difference in the germination rate between *ubc34* and wild-type plants was observed (Fig. 3A and *SI Appendix, Fig. S5*). Mutants showed stronger growth at all stages of development (Fig. 3B and *SI Appendix, Fig. S5*). Flowering time was not significantly changed from wild type (Fig. 3A). With increased SUC2 levels, photosynthesis rate, and phloem sucrose content, the phenotype of the *ubc34* mutant under normal-light conditions resembled the behavior of wild-type plants exposed to high-light conditions.

Further analysis of the *ubc34* mutant plants was performed to verify the gene's influence on the rate of SUC2 turnover. The increase in phloem exudate sucrose content in response to exposure to high-light conditions was much smaller in *ubc34* than in wild-type plants (Fig. 3C). SUC2 protein abundance showed only a slight increase that was found not to be statistically significant

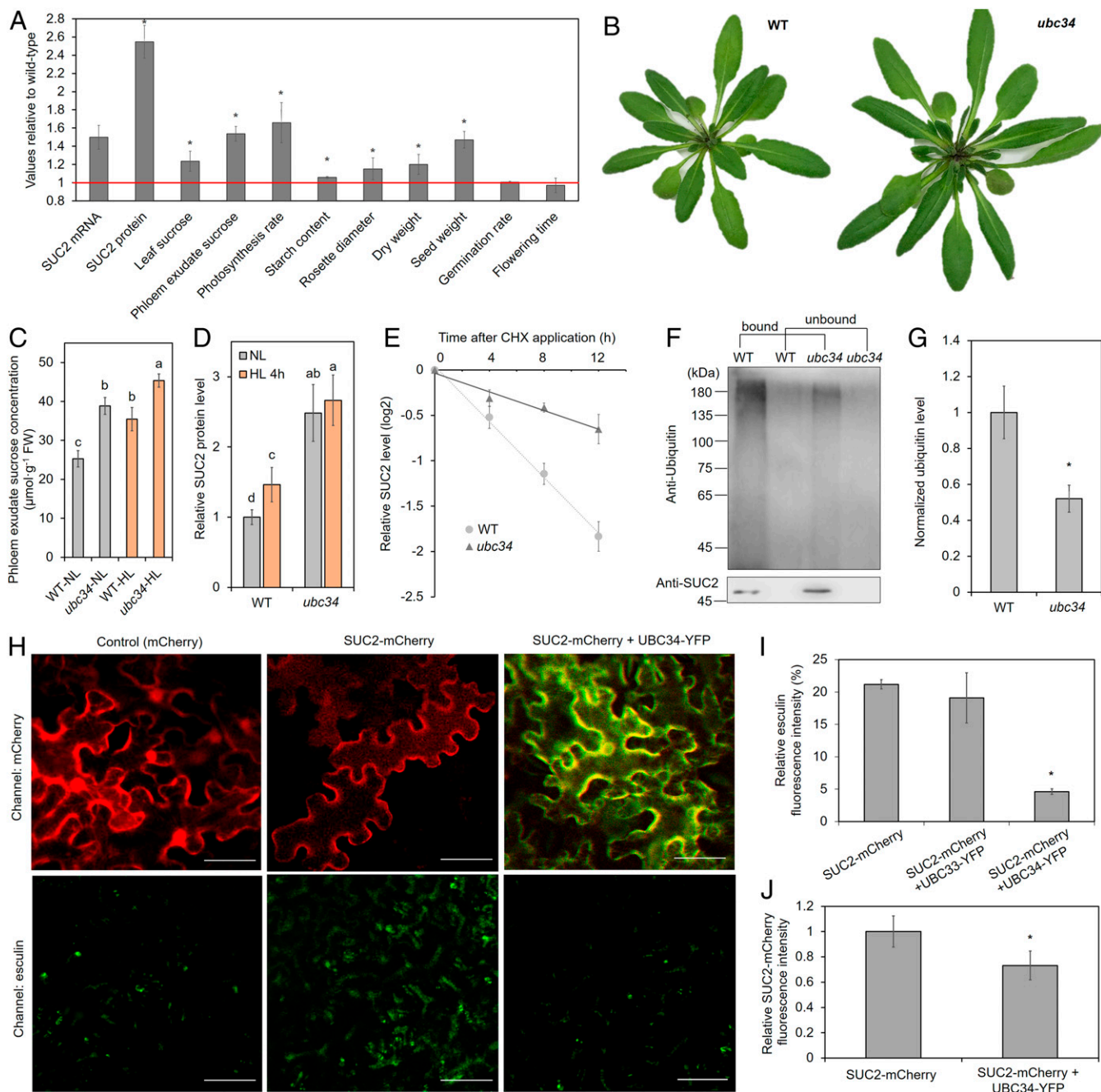


Fig. 3. UBC34-dependent degradation of SUC2. (A) Relative values of various parameters compared between 3-wk-old wild-type and *ubc34* T-DNA insertion plants. (B) Morphology of 4-wk-old wild-type and *ubc34* mutant plants. (C and D) Phloem exudate sucrose content (C) and SUC2 protein abundance (D) of 3-wk-old wild-type and *ubc34* mutant plants grown under NL or exposed to HL for 4 h. (E) Relative abundance of SUC2 protein isolated from leaves treated with cycloheximide for 4, 8, and 12 h of NL-grown wild-type and *ubc34* plants. (F) In vivo ubiquitination assay using either proteins immunoprecipitated with (bound) or without (unbound) the anti-SUC2 antibody from leaves of wild-type and *ubc34* mutant plants grown under NL. SUC2 protein levels in the immunoprecipitate are indicated (Bottom). Molecular masses are indicated as kDa. (G) Quantification of the amount of ubiquitinated SUC2 based on three replications of the ubiquitination assay. (H) Fluorescence microscopy images showing uptake of the sucrose-analog esculin in *N. benthamiana* epidermal cells expressing mCherry as negative control, SUC2-mCherry alone, or SUC2-mCherry together with UBC34-YFP. (I) Intracellular esculin signal normalized to the negative control. (J) SUC2-mCherry fluorescence signal at the cell periphery. Absolute values, additional parameters, Western blots, and images of *ubc34* plants are displayed in *SI Appendix, Figs. S4 and S5*; additional images of the esculin assay are in *SI Appendix, Fig. S7*. Significant differences ($P < 0.05$) are indicated by either asterisks or letters. Letters are arranged alphabetically starting from the highest values, with similar letters indicating no significant difference. All error bars depict SD of the mean ($n \geq 3$). (Scale bars, 50 μm .)

(Fig. 3D). These data indicate that UBC34 is important for the light-dependent increase in SUC2 levels and phloem loading. This notion was corroborated by the analysis of SUC2 abundance after application of the protein synthesis inhibitor CHX. SUC2 turnover rate in the *ubc34* mutant grown under normal light was strongly

reduced compared with wild type (Fig. 3E and *SI Appendix, Fig. S4*), resembling the turnover rate of when the whole-degradation pathway is inhibited (Fig. 1D).

Furthermore, UBC34-dependent ubiquitination of SUC2 was tested using in vitro and in vivo assays. An in vitro thioester-formation

assay confirmed the principal ability of UBC34 to bind ubiquitin (*SI Appendix, Fig. S6A*). Moreover, GST-UBC34 Δ tmd could polyubiquitinate hemagglutinin (HA)-SUC2 in vitro (*SI Appendix, Fig. S6B*). SUC2 ubiquitination in vivo was confirmed by subjecting total membrane proteins, isolated from the leaves of wild-type and *ubc34* plants, to immunoprecipitation analysis using an anti-SUC2 antibody. When probed with the anti-ubiquitin antibody, the immunoprecipitated proteins showed a smear pattern at the higher molecular masses in wild type (Fig. 3F), indicating the presence of polyubiquitinated or multimono-ubiquitinated SUC2. In *ubc34* mutants, a reduction in the signal level compared with wild type was observed (Fig. 3F). After normalization, the results showed a 48% reduction in ubiquitinated protein in *ubc34* compared with wild-type plants (Fig. 3G).

The influence of UBC34 on SUC2 activity and SUC2 abundance at the plasma membrane was investigated via heterologous expression in *N. benthamiana* leaf epidermis cells and live-cell microscopy. Esculin uptake of *N. benthamiana* leaf epidermis cells expressing SUC2-mCherry was significantly above the background fluorescence level of control cells that only express mCherry (Fig. 3H and I). When SUC2-mCherry was coexpressed with UBC34-YFP, almost no esculin uptake was observed (Fig. 3H and I). In contrast, coexpression of SUC2-mCherry with the closely related UBC33-YFP showed no significant decrease in esculin uptake compared with SUC2-mCherry expressed alone (Fig. 3I and *SI Appendix, Fig. S7*). In line with the decrease in transport activity, the signal intensity of SUC2-mCherry at the cell periphery was observed to become significantly reduced when coexpressed with UBC34-YFP (Fig. 3J). Indeed, application of the extracellular quencher trypan blue, which has a radius for energy transfer of about 5 nm and, therefore, only quenches fluorescent molecules at the plasma membrane (29), showed that significantly fewer SUC2-mCherry molecules were present at the plasma membrane when coexpressed with UBC34-YFP (*SI Appendix, Fig. S8*).

Identification of a SUC2-Regulating Kinase. While the *ubc34* mutant showed no significant increase in SUC2 protein abundance under high-light conditions (Fig. 3D), sucrose levels in exudate still showed a small but significant increase compared with normal-light conditions (Fig. 3C). As shown by Phos-Tag assay, SUC2 can be phosphorylated and the phosphorylation level was found to be significantly increased under high-light conditions (Fig. 1E). This indicates that SUC2 transport activity is regulated by a kinase. Several kinases were predicted to interact with SUC2 based on the yeast two-hybrid assay (25). This potential for interaction was confirmed here for WALL-ASSOCIATED KINASE LIKE 8 (WAKL8), CYCLIN-DEPENDENT KINASE B1;1 (CDKB1;1), and RECEPTOR-LIKE CYTOPLASMIC KINASE VII (RLCKVII)

using the FRET acceptor photobleaching method. When the acceptors WAKL8-YFP, CDKB1;1-YFP, or RLCKVII-YFP were bleached, fluorescence of the donor SUC2-mT2 significantly increased (*SI Appendix, Fig. S9*). FRET efficiencies of SUC2-mT2 with all three kinases linked to YFP were the same or higher than the positive control SUC2-mT2-SUC3-YFP (Fig. 4A). Mutants carrying T-DNA insertions in the exon or promoter sites were obtained, homozygous plants were selected by PCR-based genotyping, and the absence of gene activity was confirmed by qRT-PCR analysis (*SI Appendix, Fig. S4*). The phenotypes of these kinase mutants were then tested with regard to the ratio of SUC2 abundance and phloem loading in order to identify a kinase that could be responsible for the increased SUC2 activity under high-light conditions. Only *wakl8* showed a significantly decreased ratio of phloem sucrose content to SUC2 abundance compared with wild type (Fig. 4B and *SI Appendix, Fig. S9*), and was therefore selected for further analysis. The broad expression domain of *WAKL8* in leaves includes the phloem (Fig. 4C).

WAKL8-Dependent Phosphorylation Enhances SUC2 Activity. After confirming the principal ability of WAKL8 to phosphorylate SUC2 using an in vitro phosphorylation assay (Fig. 5A and *SI Appendix, Fig. S6 C–E*), Phos-Tag assays were used to test whether WAKL8 can phosphorylate SUC2 in vivo and if the phosphorylation level is influenced by light intensity. Like in wild type, the anti-SUC2 antibody marked an additional band on a Phos-Tag SDS polyacrylamide gel, which disappeared after treatment with alkaline phosphatase in the *wakl8* mutant (Fig. 5B and *SI Appendix, Fig. S1H*). However, the relative phosphorylation level was, at 22% (Fig. 5B), much lower than in wild type (42%) (Fig. 1E). Importantly, the phosphorylation level of SUC2 in *wakl8* mutants did not change upon exposure to high light (Fig. 5B).

A detailed analysis of the *wakl8* mutant phenotype corroborated a role of WAKL8 as a positive regulator of SUC2 transport activity. Both the SUC2 protein level and *SUC2* gene expression were similar in *wakl8* mutant and wild-type plants (Fig. 5C). At the same time, phloem exudate sucrose content was reduced by about 50% (Fig. 5C). Photosynthesis rate and leaf sugar levels were significantly reduced as well (Fig. 5C and *SI Appendix, Fig. S5*). Consequently, mutants showed reduced growth and yield (Fig. 5C and D and *SI Appendix, Fig. S5*), while germination rate and flowering time were not significantly changed (Fig. 5C). High-light treatment still led to significantly higher phloem exudate sucrose concentrations, but the increase was smaller compared with the wild-type plants (Fig. 5E). The phloem exudate sucrose level in *wakl8* under high-light conditions remained below the concentration in wild-type plants under

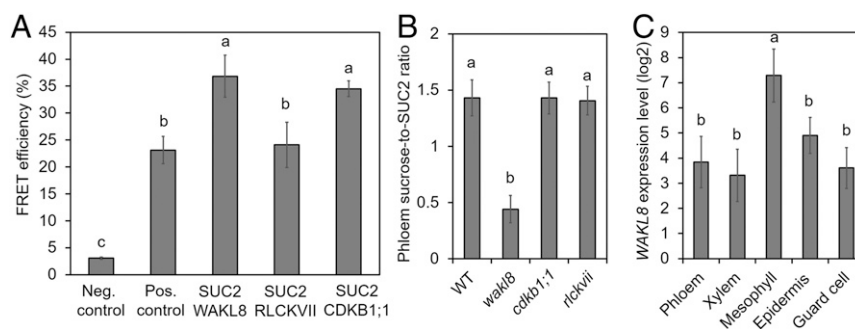


Fig. 4. Protein–protein interaction of kinases and SUC2. (A) FRET efficiency of SUC2-mT2 and, respectively, WAKL8-YFP, RLCKVII-YFP, and CDKB1;1-YFP compared with efficiency of the negative control SUC2-mT2 and STP1-YFP and the positive control SUC2-mT2 and SUC3-YFP. (B) Ratio of phloem exudate sucrose content to SUC2 protein abundance in wild-type and *wakl8*, *rlckvii*, and *cdkb1;1* mutant plants. (C) Relative gene expression of *WAKL8* in different tissues of rosette leaves. Representative images of FRET experiments, Western blots, and phloem exudate sucrose concentrations are displayed in *SI Appendix, Fig. S9*. Significant differences ($P < 0.05$) are indicated by letters, which are arranged alphabetically starting from the highest values, with similar letters indicating no significant difference. All error bars depict SD of the mean ($n = 3$).

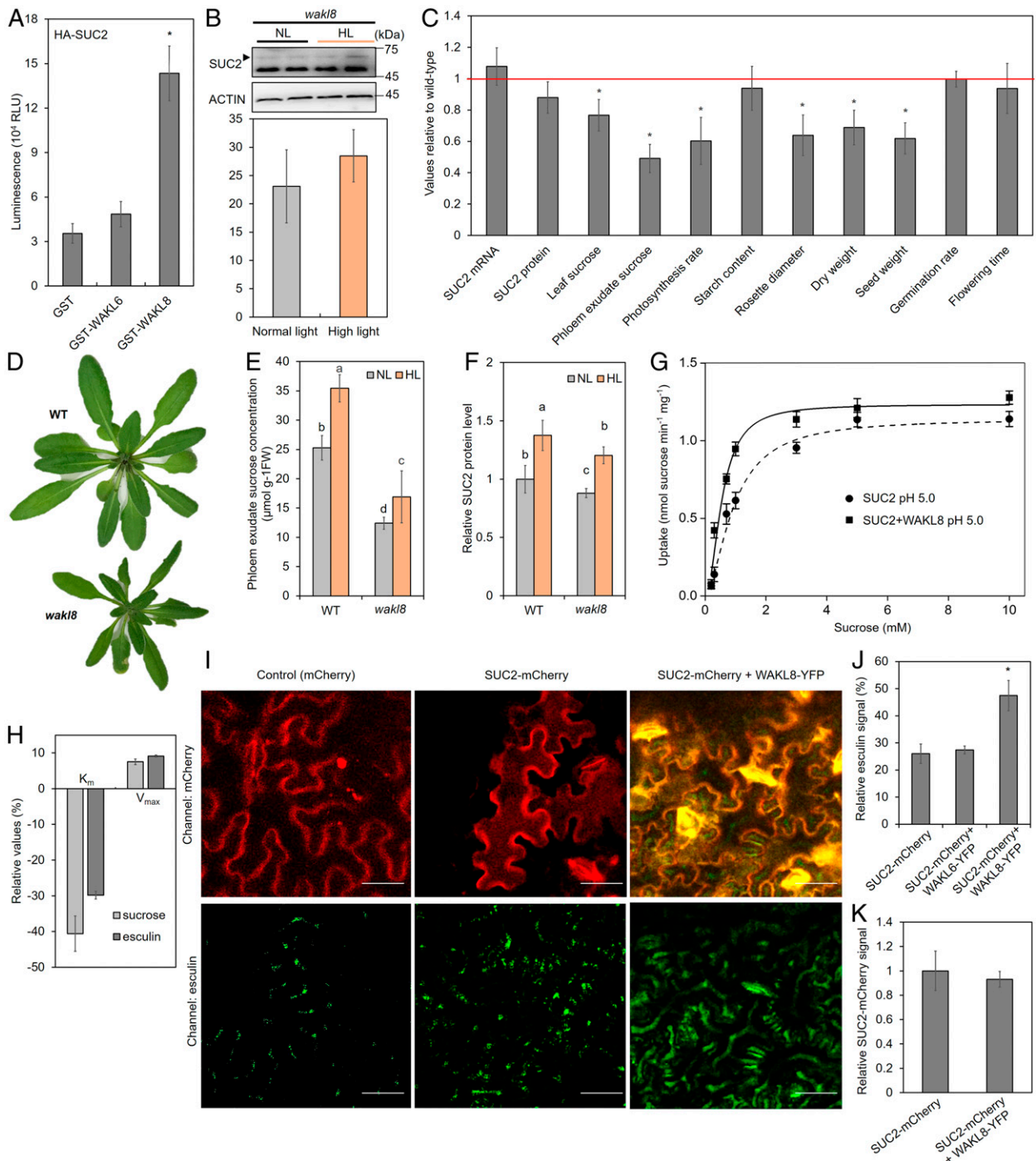


Fig. 5. SUC2-related parameters and traits of the *wak18* T-DNA insertion mutant and influence of WAKL8 on SUC2 activity. (A) In vitro phosphorylation assay of SUC2 and WAKL8, in which luminescence (in relative luminescence units; RLU) indicates the ADP production that results from the phosphorylation reaction. GST and GST-WAKL6 are used as negative controls. (B, Upper) Immunoblot analysis of the *wak18* mutant with a SUC2 antibody using Phos-Tag SDS/PAGE. The triangle indicates bands of phosphorylated SUC2 protein. (B, Lower) The relative amount of phosphorylated SUC2 protein under normal- and high-light conditions. (C) Relative values of various parameters compared between 3-wk-old wild-type and *wak18* plants. Absolute values, additional parameters, and images of the *wak18* mutant are displayed in *SI Appendix, Fig. S5*. (D) Morphology of 4-wk-old wild-type and *wak18* mutant plants. (E) Phloem exudate sucrose content of 3-wk-old wild-type and *wak18* mutant plants grown under NL or exposed to HL for 4 h. Concentrations of other sugars are shown in *SI Appendix, Fig. S5*. (F) Relative SUC2 protein level in leaves of wild-type and *wak18* mutant plants grown under NL or exposed to HL. (G) Uptake of ^{13}C -labeled sucrose in a sucrose uptake-deficient yeast strain complemented with SUC2 or complemented with SUC2 and coexpressing WAKL8, measured at pH 5. Lines represent nonlinear regression fits of the Michaelis–Menten equation. The corresponding plot with esculin as substrate is shown in *SI Appendix, Fig. S11*. (H) Relative K_m and V_{max} of yeast cells expressing SUC2 alone or coexpressing SUC2 and WAKL8 measured with either sucrose or esculin as substrate. (I) Fluorescence images indicating uptake of the sucrose-analog esculin in *N. benthamiana* epidermal cells expressing mCherry as negative control, SUC2-mCherry alone, or SUC2-mCherry together with WAKL8-YFP visualized by fluorescence microscopy. Corresponding images with the negative control WAKL8-YFP are shown in *SI Appendix, Fig. S7*. (J) Intracellular esculin signal normalized to the negative control. (K) SUC2-mCherry fluorescence signal at the cell periphery. Significant difference ($P < 0.05$) is indicated by either asterisks or letters. Letters are arranged alphabetically starting from the highest values, with similar letters indicating no significant difference. All error bars depict SD of the mean ($n \geq 3$ [A–C, E, and H] and 5 [J and K]). (Scale bars, 50 μm .)

normal-light conditions (Fig. 5E), even though there was no significant difference in the abundance of SUC2 protein (Fig. 5F).

The effect of WAKL8 on SUC2-mediated transport was further characterized by heterologous expression in sucrose uptake-deficient yeast cells. On medium containing sucrose as the sole carbon source, yeast cells coexpressing SUC2 and WAKL8 grew faster than those expressing SUC2 alone (SI Appendix, Fig. S10). In contrast, coexpression of WAKL8 with SUC1 did not influence growth (SI Appendix, Fig. S10), indicating that WAKL8 affects SUC2 activity directly instead of indirectly, for example, via increasing the proton motive force. This was confirmed by measuring proton uptake in plasma membrane vesicles derived either from yeast cells expressing SUC2 alone or coexpressing SUC2 and WAKL8 and finding no significant difference (SI Appendix, Fig. S11A). The effect of WAKL8 on the kinetics of SUC2-mediated transport was determined by measuring the uptake of ^{13}C -labeled sucrose (Fig. 5G and SI Appendix, Fig. S11B and C). Coexpression with WAKL8 decreased the K_m by 40% and increased the V_{max} by 8% (Fig. 5H), indicating that phosphorylation primarily affects the substrate affinity of SUC2. Measuring esculin uptake instead of sucrose uptake yielded higher values for K_m and V_{max} (SI Appendix, Fig. S11B–D), but the relative effect of WAKL8 expression on SUC2 transport kinetics was not significantly different (Fig. 5H), and SUC2 showed a similar pH dependence with esculin or sucrose as substrate (SI Appendix, Fig. S11E).

With the suitability of esculin for SUC2-activity studies confirmed, the effect of WAKL8 on SUC2 activity was investigated in planta. WAKL6, a close relative of WAKL8, was included as negative control. When SUC2-mCherry and WAKL8-YFP were coexpressed in the same *N. benthamiana* leaf epidermis cells, esculin uptake increased by about 80% compared with when SUC2-mCherry was expressed alone (Fig. 5I and J). No significant change was observed when coexpressed with WAKL6-YFP (Fig. 5J and SI Appendix, Fig. S7). The fluorescence intensity of SUC2-mCherry at the cell periphery was not affected by coexpression with WAKL8-YFP (Fig. 5K). Accordingly, application of the extracellular quencher trypan blue indicated the same accessibility of SUC2-mCherry with or without coexpression of WAKL8-mT2 (SI Appendix, Fig. S8). The results demonstrate that WAKL8 can phosphorylate SUC2 to increase transport activity and indicate a contribution of this regulatory mechanism to the high light-dependent increase in phloem loading.

Discussion

Sucrose loading into the phloem in leaves is a key step in whole-plant carbon partitioning. If a plant encounters favorable conditions that allow for increased photosynthesis, it also needs to increase phloem loading to keep the balance between source and sink (30). The identification of UBC34 and WAKL8 as regulators of SUC2 provides insight into the molecular mechanism of how the rate of carbon export from leaves is adjusted.

SUC2 regulation via modulation of protein turnover rate agrees with previous reports, which concluded that SUCs are relatively short-lived, unstable proteins (9, 31). Nevertheless, the mode of regulation is remarkable, because UBC34 is an E2 enzyme (32). According to textbook knowledge, E2 enzymes are only responsible for providing ubiquitin to E3 ubiquitin ligases, which recognize the target protein and attach the ubiquitin (33). Here, UBC34 is shown to specifically interact with SUC2 and to facilitate SUC2 ubiquitination in vitro. Together with the recent report of the E2 ubiquitin-conjugating enzyme UBC32 regulating processivity and specificity of AtOS9 turnover (34), these results demonstrate an enhanced capability of E2 enzymes in plants.

The *ubc34* mutant phenotype with its higher light-use efficiency compared with wild-type plants indicates that SUC-regulatory factors might be better targets for the improvement of plant productivity than SUCs themselves. In various dicots, overexpression of the SUC responsible for phloem loading never

led to significant increases of photosynthesis or yield (35–38). A yield increase was only observed when *Arabidopsis* SUC2 was overexpressed in rice, presumably because the dicot SUC is not affected by regulatory mechanisms of monocot SUCs (39). It should be noted that UBC34 is likely to regulate other proteins in addition to SUC2, since the interactomics screen by Jones et al. (25) indicated over 100 potential interaction partners. Moreover, the *ubc34* mutant phenotype hints at additional target proteins, as it displayed coregulation of phloem loading and photosynthetic sugar production. Previously analyzed mutants deficient in phloem loading, in contrast, were shown to accumulate sugars in the leaf (2). Investigation of potential interaction partners will be essential to understand how UBC34 fulfills its apparent role as master regulator of growth.

With regard to the control of *UBC34*, it was found that its promoter contains four predicted binding sites for the GBF6 transcription factor (40), which is light-regulated (41) and can act as a sucrose sensor (42). This provides an exciting hypothesis for the long-proposed link between sucrose levels and SUC2 activity (8, 43).

Of the mutants of the three kinases that interacted with SUC2, RLCKVII and CDKB1;1 showed no change in SUC2 activity. In these cases, phosphorylation might serve as a signal, for example for SUC2 internalization and/or turnover, instead of directly affecting SUC2 function. Alternatively, they might be involved in responses other than high-light acclimation. Only WAKL8 affected SUC2 function and was found to be involved in the high light-dependent up-regulation of phloem loading. Members of the *WAK/WAKL* gene family have been primarily implicated in signaling during cell expansion and pathogen attack (44–46). While WAKs were shown to bind pectin in the cell wall (44), it is unclear if WAKLs can directly interact with wall components, as their extracellular domain differs with regard to the proposed pectin binding site (47). In the absence of clear evidence for WAKL ligands, it can only be speculated as to what signal stimulates WAKL8 activity and, in turn, affects SUC2 function. The extracellular part of WAKLs contains an EGF-like calcium-binding domain (45), potentially indicating a link to Ca^{2+} -dependent regulation of phloem transport (48). Moreover, several WAKLs were shown to react to wounding-related signals, including reactive oxygen species (45). Reactive oxygen species and other redox agents have been identified as important factors for the acclimation of *Arabidopsis* plants to high-light conditions (49), and redox-dependent regulation of SUCs was indicated previously (50).

That *ubc34* as well as *wakl8* mutants both displayed a moderate high light-dependent up-regulation of phloem loading indicates that both pathways act, at least partly, independent from each other. Understanding their upstream control will be the next step toward complete understanding of the molecular regulation of carbon export from leaves.

Materials and Methods

Arabidopsis (accession Col-0) wild type and mutants were grown in growth chambers with a 16-h light/8-h dark cycle at $90 \mu\text{mol photon}\cdot\text{m}^{-2}\cdot\text{s}^{-1}$ and 22°C . For high-light treatment, the light intensity was increased to $400 \mu\text{mol photon}\cdot\text{m}^{-2}\cdot\text{s}^{-1}$ and samples were collected after 4 h. Measurements of photosynthesis, leaf sugar levels, starch levels, phloem exudate sugar concentrations, gene expression, and protein abundance followed standard protocols described in SI Appendix, Materials and Methods. For FRET, esculin, and quenching assays, the vectors pGWB444, pGWB441, and pB121 were modified to include the proteins of interest and either YFP, mT2, or mCherry, and transformed into *N. benthamiana* with the help of *Agrobacterium tumefaciens* strain GV3101. FRET experiments followed the standard protocol for acceptor photobleaching. The quenching assay was performed by adding $40 \mu\text{M}$ trypan blue solution to *N. benthamiana* cells expressing the protein of interest fused to YFP and recording the intensity change within 5 min. For measuring esculin uptake in transformed *N. benthamiana* cells, 2-cm^2 pieces of a leaf were soaked in 1 mM esculin solution for 10 min before analysis by a confocal microscope. Proteins of interest were purified after expression in

E. coli using the GST tag (UBC34Δtmd, WAKL8, WAKL6) or in yeast using the HA tag (SUC2). These purified proteins were used for pull-down, thioester, in vitro ubiquitination, and in vitro phosphorylation assays that were performed according to standard protocols. Immunoprecipitation and in vivo ubiquitination assays were performed by extracting *Arabidopsis* leaf membrane proteins followed by immunoprecipitation using an affinity-purified anti-SUC2 antibody and immunoblot analysis. Ubiquitination of the immunoprecipitated proteins was detected using a monoclonal anti-ubiquitin antibody. Total membrane proteins were also used to detect phosphorylated SUC2 by using the proteins for SDS polyacrylamide gel electrophoresis (PAGE) in the presence of 20 μM Mn²⁺-Phos-Tag. After electrophoretic separation, the gels were incubated in transfer buffer containing 10 mM EDTA for at least 10 min four times and then in transfer buffer without EDTA for an additional 10 min. For yeast-complementation assays, SUC2, SUC1, and WAKL8 were cloned into the pDR196 vector and transformed into the yeast strain SUSY7/ura3⁻, which lacks the sucrose synthase necessary for efficient growth on sucrose medium. Assessment of yeast growth was performed on minimal selective medium at pH 5.0 supplemented with sucrose (2%, wt/vol) or glucose (2%, wt/vol) as the sole carbon source. Sucrose-uptake experiments were performed with

¹³C-labeled sucrose, which was supplied at various concentrations for 5 min, at pH 5. After vacuum freeze drying the yeast cells, their ¹³C content was analyzed using isotope ratio mass spectrometry and elemental analysis. A kinetic analysis of SUC2 activity in yeast was also performed using esculin as substrate in the same way as for sucrose, only that, after 5 min of incubation, uptake was directly determined as fluorescence intensity at 454 nm measured on a spectrofluorometer. Proton flux across yeast plasma membrane vesicles was performed as described previously (10). Detailed descriptions of experimental procedures are provided in *SI Appendix, Materials and Methods*.

Data Availability Statement. All data underlying the study are available in the paper or *SI Appendix*.

ACKNOWLEDGMENTS. We thank Prof. Wolf Frommer (Heinrich Heine University Düsseldorf) for critical reading of the manuscript and input toward the project; as well as Prof. Legong Li (Beijing Capital University) and Prof. Cun Wang (Northwest A&F University) for their advice regarding the measurement of transport kinetics. Microscopic imaging was performed at Northwest A&F University's Life Science Core Services facility.

1. A. M. Smith, M. Stitt, Coordination of carbon supply and plant growth. *Plant Cell Environ.* **30**, 1126–1149 (2007).
2. J. Liesche, J. Patrick, An update on phloem transport: A simple bulk flow under complex regulation. *F1000 Res.* **6**, 2096 (2017).
3. D. M. Braun, Plant science. SWEET! The pathway is complete. *Science* **335**, 173–174 (2012).
4. T. J. Ross-Elliott et al., Phloem unloading in *Arabidopsis* roots is convective and regulated by the phloem-pole pericycle. *eLife* **6**, e24125 (2017).
5. M. Durand et al., Carbon source-sink relationship in *Arabidopsis thaliana*: The role of sucrose transporters. *Planta* **247**, 587–611 (2018).
6. K. Knox, A. Paterlini, S. Thomson, K. Oparka, The coumarin glucoside, esculin, reveals rapid changes in phloem-transport velocity in response to environmental cues. *Plant Physiol.* **178**, 795–807 (2018).
7. Q. Xu, S. Chen, R. Yunjuan, S. Chen, J. Liesche, Regulation of sucrose transporters and phloem loading in response to environmental cues. *Plant Physiol.* **176**, 930–945 (2018).
8. T. J. Chiou, D. R. Bush, Sucrose is a signal molecule in assimilate partitioning. *Proc. Natl. Acad. Sci. U.S.A.* **95**, 4784–4788 (1998).
9. M. W. Vaughn, G. N. Harrington, D. R. Bush, Sucrose-mediated transcriptional regulation of sucrose symporter activity in the phloem. *Proc. Natl. Acad. Sci. U.S.A.* **99**, 10876–10880 (2002).
10. U. Krügel et al., Transport and sorting of the *Solanum tuberosum* sucrose transporter SUT1 is affected by posttranslational modification. *Plant Cell* **20**, 2497–2513 (2008).
11. J. Liesche, H. X. He, B. Grimm, A. Schulz, C. Kühn, Recycling of solanum sucrose transporters expressed in yeast, tobacco, and in mature phloem sieve elements. *Mol. Plant* **3**, 1064–1074 (2010).
12. I. A. Chincinska et al., Sucrose transporter StSUT4 from potato affects flowering, tuberization, and shade avoidance response. *Plant Physiol.* **146**, 515–528 (2008).
13. A. Reinders et al., Protein-protein interactions between sucrose transporters of different affinities localized in the same enucleated sieve element. *Plant Cell* **14**, 1567–1577 (2002).
14. E. Eggert et al., A sucrose transporter-interacting protein disulphide isomerase affects redox homeostasis and links sucrose partitioning with abiotic stress tolerance. *Plant Cell Environ.* **39**, 1366–1380 (2016).
15. U. Krügel et al., The potato sucrose transporter StSUT1 interacts with a DRM-associated protein disulfide isomerase. *Mol. Plant* **5**, 43–62 (2012).
16. W. D. Ransom-Hodgkins, M. W. Vaughn, D. R. Bush, Protein phosphorylation plays a key role in sucrose-mediated transcriptional regulation of a phloem-specific proton-sucrose symporter. *Planta* **217**, 483–489 (2003).
17. G. Roblin, S. Sakr, J. Bonmort, S. Delrot, Regulation of a plant plasma membrane sucrose transporter by phosphorylation. *FEBS Lett.* **424**, 165–168 (1998).
18. T. S. Nühse, A. Stensballe, O. N. Jensen, S. C. Peck, Phosphoproteomics of the *Arabidopsis* plasma membrane and a new phosphorylation site database. *Plant Cell* **16**, 2394–2405 (2004).
19. T. Niittylä, A. T. Fuglsang, M. G. Palmgren, W. B. Frommer, W. X. Schulze, Temporal analysis of sucrose-induced phosphorylation changes in plasma membrane proteins of *Arabidopsis*. *Mol. Cell. Proteomics* **6**, 1711–1726 (2007).
20. Q. J. Ma et al., A CIPK protein kinase targets sucrose transporter MdsUT2.2 at Ser²⁵⁴ for phosphorylation to enhance salt tolerance. *Plant Cell Environ.* **42**, 918–930 (2019).
21. Q. J. Ma et al., An apple sucrose transporter MdsUT2.2 is a phosphorylation target for protein kinase MdCIPK22 in response to drought. *Plant Biotechnol. J.* **17**, 625–637 (2019).
22. E. Truernit, N. Sauer, The promoter of the *Arabidopsis thaliana* SUC2 sucrose-H⁺ symporter gene directs expression of beta-glucuronidase to the phloem: Evidence for phloem loading and unloading by SUC2. *Planta* **196**, 564–570 (1995).
23. R. Stadler, N. Sauer, The *Arabidopsis thaliana* AtSUC2 gene is specifically expressed in companion cells. *Bot. Acta* **109**, 261–340 (1996).
24. J. R. Gottwald, P. J. Krysan, J. C. Young, R. F. Evert, M. R. Sussman, Genetic evidence for the in planta role of phloem-specific plasma membrane sucrose transporters. *Proc. Natl. Acad. Sci. U.S.A.* **97**, 13979–13984 (2000).
25. A. M. Jones et al., Border control—A membrane-linked interactome of *Arabidopsis*. *Science* **344**, 711–716 (2014).
26. T. M. Rottmann et al., Protoplast-esculin assay as a new method to assay plant sucrose transporters: Characterization of AtSUC6 and AtSUC7 sucrose uptake activity in *Arabidopsis* Col-0 ecotype. *Front. Plant Sci.* **9**, 430 (2018).
27. J. Paez Valencia, K. Goodman, M. S. Otegui, Endocytosis and endosomal trafficking in plants. *Annu. Rev. Plant Biol.* **67**, 309–335 (2016).
28. M. Barberon et al., Monoubiquitin-dependent endocytosis of the iron-regulated transporter 1 (IRT1) transporter controls iron uptake in plants. *Proc. Natl. Acad. Sci. U.S.A.* **108**, E450–E458 (2011).
29. X. Liu et al., Novel tool to quantify cell wall porosity relates wall structure to cell growth and drug uptake. *J. Cell Biol.* **218**, 1408–1421 (2019).
30. A. C. White, A. Rogers, M. Rees, C. P. Osborne, How can we make plants grow faster? A source-sink perspective on growth rate. *J. Exp. Bot.* **67**, 31–45 (2016).
31. C. Kühn, V. R. Franceschi, A. Schulz, R. Lemoine, W. B. Frommer, Macromolecular trafficking indicated by localization and turnover of sucrose transporters in enucleate sieve elements. *Science* **275**, 1298–1300 (1997).
32. M. Y. Ahn et al., *Arabidopsis* group XIV ubiquitin-conjugating enzymes AtUBC32, AtUBC33, and AtUBC34 play negative roles in drought stress response. *J. Plant Physiol.* **230**, 73–79 (2018).
33. J. Smalle, R. D. Vierstra, The ubiquitin 26S proteasome proteolytic pathway. *Annu. Rev. Plant Biol.* **55**, 555–590 (2004).
34. Q. Chen, R. Liu, Q. Wang, Q. Xie, ERAD tuning of the HRD1 complex component AtOS9 is modulated by an ER-bound E2, UBC32. *Mol. Plant* **10**, 891–894 (2017).
35. G. Leggewie et al., Overexpression of the sucrose transporter SoSUT1 in potato results in alterations in leaf carbon partitioning and in tuber metabolism but has little impact on tuber morphology. *Planta* **217**, 158–167 (2003).
36. A. C. Srivastava, S. Ganesan, I. O. Ismail, B. G. Ayre, Effective carbon partitioning driven by exotic phloem-specific regulatory elements fused to the *Arabidopsis thaliana* AtSUC2 sucrose-proton symporter gene. *BMC Plant Biol.* **9**, 7 (2009).
37. E. Gabriel-Neumann, G. Neumann, G. Leggewie, E. George, Constitutive overexpression of the sucrose transporter SoSUT1 in potato plants increases arbuscular mycorrhiza fungal root colonization under high, but not under low, soil phosphorus availability. *J. Plant Physiol.* **168**, 911–919 (2011).
38. K. Dasgupta et al., Expression of sucrose transporter cDNAs specifically in companion cells enhances phloem loading and long-distance transport of sucrose but leads to an inhibition of growth and the perception of a phosphate limitation. *Plant Physiol.* **165**, 715–731 (2014).
39. L. Wang, Q. Lu, X. Wen, C. Lu, Enhanced sucrose loading improves rice yield by increasing grain size. *Plant Physiol.* **169**, 2848–2862 (2015).
40. A. Yilmaz et al., AGRIS: The *Arabidopsis* Gene Regulatory Information Server, an update. *Nucleic Acids Res.* **39**, D1118–D1122 (2011).
41. F. Rook et al., Sucrose-specific signalling represses translation of the *Arabidopsis* ATB2 bZIP transcription factor gene. *Plant J.* **15**, 253–263 (1998).
42. Y. Yamashita et al., Sucrose sensing through nascent peptide-mediated ribosome stalling at the stop codon of *Arabidopsis* bZIP11 uORF2. *FEBS Lett.* **591**, 1266–1277 (2017).
43. L. Li, J. Sheen, Dynamic and diverse sugar signaling. *Curr. Opin. Plant Biol.* **33**, 116–125 (2016).
44. C. M. Anderson et al., WAKs: Cell wall-associated kinases linking the cytoplasm to the extracellular matrix. *Plant Mol. Biol.* **47**, 197–206 (2001).
45. J. A. Verica, L. Chae, H. Tong, P. Ingmire, Z. H. He, Tissue-specific and developmentally regulated expression of a cluster of tandemly arrayed cell wall-associated kinase-like kinase genes in *Arabidopsis*. *Plant Physiol.* **133**, 1732–1746 (2003).
46. E. Häffner, P. Karlovsky, R. Splivallo, A. Traczewska, E. Diederichsen, ERECTA, salicylic acid, abscisic acid, and jasmonic acid modulate quantitative disease resistance of *Arabidopsis thaliana* to *Verticillium longisporum*. *BMC Plant Biol.* **14**, 85 (2014).
47. X. Hou et al., Involvement of a cell wall-associated kinase, WAKL4, in *Arabidopsis* mineral responses. *Plant Physiol.* **139**, 1704–1716 (2005).
48. A. J. van Bel et al., Spread the news: Systemic dissemination and local impact of Ca²⁺ signals along the phloem pathway. *J. Exp. Bot.* **65**, 1761–1787 (2014).
49. K. Alsharafa et al., Kinetics of retrograde signalling initiation in the high light response of *Arabidopsis thaliana*. *Philos. Trans. R. Soc. Lond. B Biol. Sci.* **369**, 20130424 (2014).
50. C. Kühn, C. P. Grof, Sucrose transporters of higher plants. *Curr. Opin. Plant Biol.* **13**, 288–298 (2010).